© 2014. Published by The Company of Biologists Ltd | Journal of Cell Science (2014) 127, 1924–1937 doi:10.1242/jcs.139337

RESEARCH ARTICLE

Specific recycling receptors are targeted to the immune synapse by the intraflagellar transport system

Francesca Finetti[1], Laura Patrussi[1], Giulia Masi[1], Anna Onnis[1], Donatella Galgano[1], Orso Maria Lucherini[1], Gregory J. Pazour[2] and Cosima T. Baldari[1,*]

ABSTRACT

T cell activation requires sustained signaling at the immune synapse, a specialized interface with the antigen-presenting cell (APC) that assembles following T cell antigen receptor (TCR) engagement by major histocompatibility complex (MHC)-bound peptide. Central to sustained signaling is the continuous recruitment of TCRs to the immune synapse. These TCRs are partly mobilized from an endosomal pool by polarized recycling. We have identified IFT20, a component of the intraflagellar transport (IFT) system that controls ciliogenesis, as a central regulator of TCR recycling to the immune synapse. Here, we have investigated the interplay of IFT20 with the Rab GTPase network that controls recycling. We found that IFT20 forms a complex with Rab5 and the TCR on early endosomes. IFT20 knockdown (IFT20KD) resulted in a block in the recycling pathway, leading to a build-up of recycling TCRs in Rab5$^+$ endosomes. Recycling of the transferrin receptor (TfR), but not of CXCR4, was disrupted by IFT20 deficiency. The IFT components IFT52 and IFT57 were found to act together with IFT20 to regulate TCR and TfR recycling. The results provide novel insights into the mechanisms that control TCR recycling and immune synapse assembly, and underscore the trafficking-related function of the IFT system beyond ciliogenesis.

KEY WORDS: Intraflagellar transport, Immune synapse, Receptor recycling, Rab GTPases, Receptor sorting

INTRODUCTION

T cell activation is dependent on the assembly of a highly organized membrane domain that forms at the interface with the antigen-presenting cell (APC). This domain is known as the immune synapse, and it assembles in response to the engagement of the T cell antigen receptor (TCR) by peptide antigen associated with the major histocompatibility complex (MHC). This specialized membrane domain acts as a platform where the signals from the TCR, as well as from the co-stimulatory receptors and adhesion molecules that are recruited to this location, are integrated to initiate and coordinate the cell-activation program (Fooksman et al., 2010). The immune synapse ensures sustained signaling, on which T cell activation crucially depends (Iezzi et al., 1998), by promoting the steady recruitment of new TCR complexes as engaged TCRs undergo receptor-mediated endocytosis.

It was initially thought that TCR recruitment to the immune synapse involved both passive and actin-driven lateral motility of surface TCRs towards the center of the immune synapse; however, it is now clear that a major proportion of the TCR complexes that cluster to the immune synapse is mobilized from an intracellular pool associated with recycling endosomes, undergoing delivery to the immune synapse membrane through microtubule-dependent polarized recycling (Das et al., 2004). Recent findings have demonstrated that this mechanism of recruitment to the immune synapse is not unique to the TCR. The transferrin receptor (TfR), a major recycling receptor, also polarizes to the immune synapse in CD4$^+$ T cells, and it contributes to the stability of the immune synapse (Batista et al., 2004). Moreover, LCK and LAT, two central participants in TCR signaling, are stored in part in an endosomal pool, wherefrom they are delivered to the immune synapse with delayed kinetics compared with protein associated with the plasma membrane, thereby contributing to sustained signaling (Ehrlich et al., 2002; Bonello et al., 2004). Regulators of vesicular trafficking, such as Rab35 and its GTPase-activating protein (GAP) EPI64C (also known as TBC1D10C) (Patino-Lopez et al., 2008), the SNAREs SNAP-23, syntaxin-4, VAMP-3 (Das et al., 2004) and VAMP-7 (Larghi et al., 2013; Soares et al., 2013), and the adaptor UNC-119 (Gorska et al., 2009) are also recruited to the immune synapse, highlighting the immune synapse as a site of polarized endosomal trafficking.

Our understanding of the molecular players that regulate vesicular trafficking to the immune synapse is currently limited. We have recently identified IFT20, a component of the intraflagellar transport system (Pazour and Bloodgood, 2008), as a regulator of TCR recycling (Finetti et al., 2009). In ciliated cells, IFT20 participates in the transport of ciliary proteins across the periciliary barrier into the cilium, acting as a component of a particle that includes several IFT polypeptides (Pedersen and Rosenbaum, 2008; Baldari and Rosenbaum, 2010). Based on its dual ciliary and Golgi localization (Follit et al., 2006), IFT20 has been proposed to mark membrane proteins that are destined for primary cilia during their sorting at the Golgi and to assist their delivery to the cilium. This notion has been substantiated for the traffic of opsin to the photoreceptor outer segment, which is a specialized cilium (Keady et al., 2011). Recently, other IFT polypeptides, such as IFT52 and IFT57, have been found to display not only a ciliary, but also a vesicular, localization (Sedmak and Wolfrum, 2010). Taken together with bioinformatic data that highlight structural similarities between IFT proteins and components of membrane coats (Jékely and Arendt, 2006), these results strongly support the notion that the IFT system might represent a previously unidentified player in vesicular trafficking, beyond its role in ciliogenesis.

[1]Department of Life Sciences, University of Siena, 53100 Siena, Italy. [2]Program in Molecular Medicine, University of Massachusetts Medical School, Worcester, MA 01605, USA.

*Author for correspondence (cosima.baldari@unisi.it)

Received 26 July 2013; Accepted 27 January 2014

Journal of Cell Science

Journal of Cell Science (2014) 127, 1924–1937 doi:10.1242/jcs.139337

Previously, we showed that, in T cells, which lack primary cilia, IFT20 associates with a number of vesicular compartments and is required both for constitutive TCR recycling and for polarized recycling of the TCR to the immune synapse (Finetti et al., 2009). Here, we have asked how IFT20 interfaces with the Rab GTPase network that orchestrates receptor recycling to control TCR trafficking, and whether the IFT system selectively controls the recycling of specific receptors to the immune synapse. The results provide evidence that IFT20 has a role in TCR sorting and/or trafficking from early endosomes, and that it functions by forming a complex with Rab5. Moreover, they show that IFT20, acting in concert with two other components of the IFT system, coordinates a pathway that is selectively exploited by specific receptors to undergo polarized recycling to the immune synapse.

RESULTS

IFT20 colocalizes with Rab4, Rab5 and Rab11 in T cells

Following their internalization, recycling receptors are sorted from $Rab5^+$ early endosomes to be redirected to the cell surface in $Rab4^+$ endosomes. Alternatively, they are targeted to the $Rab11^+$ pericentrosomal compartment, wherefrom they are recycled to the cell surface using a longer route (Hutagalung and Novick, 2011). To map IFT20 within the recycling pathway, the colocalization of IFT20 with Rab5, Rab4 and Rab11 was investigated by using confocal microscopy in Jurkat T cells and normal peripheral T cells transfected with Rab–GFP constructs. Rab7, which marks late endosomes, was included as a recycling-unrelated control. IFT20 displayed substantial colocalization with Rab4, as well as with Rab11 and Rab5, and only a minor colocalization with Rab7 (Fig. 1A,B; supplementary material Fig. S1A).

Within the scant T cell cytosol, early and recycling Rabs are largely concentrated at a pericentrosomal location that is also occupied by the Golgi complex and, indeed, some overlap of GFP-tagged Rab4, Rab5 and Rab11 with the cis-Golgi marker GM130 could be observed (data not shown). Hence, the association of IFT20 with early and recycling endosomes was also addressed biochemically by using immunoblot analysis of cell membranes following iodixanol gradient fractionation. Early and recycling endosomes segregated to the low-density fractions, as assessed by probing with antibodies against Rab4, Rab5 and Rab11, whereas late endosomes, identified by Rab7, were found in higher-density fractions. Because the largest proportion of IFT20 is associated with the Golgi complex in T cells (Finetti et al., 2009; Fig. 1C), fractions were also probed with antibodies against GM130, which, similar to Rab7, was detected in intermediate-to-high density fractions. IFT20 showed a bimodal distribution, with a modest but distinct enrichment in low-density fractions that were enriched in early and recycling endosomes and a more substantial enrichment in higher density fractions (Fig. 1C). Based on the colocalization analyses showing only a minor association of IFT20 with Rab7 (Fig. 1A), as well as the very distinct staining pattern of GM130 and Rab7 (Fig. 1C), the IFT20 pool present in the intermediate-to-high density fractions can be accounted for by its association with the Golgi complex. Collectively, these data confirm an association of a pool of IFT20 with early and recycling endosomes, and support the notion that IFT20 regulates endosome recycling by interfacing with the Rab-based trafficking machinery.

IFT20 interacts with Rab5 at the level of early endosomes

The ability of IFT20 to interact with the Rab GTPases that are associated with early and recycling endosomes was assessed in co-immunoprecipitation experiments, using a Jurkat T cell transfectant that expressed GFP-tagged IFT20. IFT20 was found to interact with Rab5. By contrast, only a minimal interaction of IFT20 with Rab11 and Rab4, and none with Rab7, was found (Fig. 2A). The interaction of IFT20 with Rab5 was confirmed in Rab5-specific co-immunoprecipitation assays (Fig. 2B). Of note, the TCR was found to co-precipitate with Rab5 in activated control cells and, to a small extent, in unstimulated cells (longer exposure, not shown), as assessed by immunoblot with anti-CD3ζ and anti-CD3ε antibodies. This interaction was impaired in cells that were stably knocked down for IFT20 expression [>75% IFT20 knockdown (IFT20KD); examples shown in supplementary material Fig. S1B] (Fig. 2B). Taken together with the ability of IFT20 to interact with the TCR (Finetti et al., 2009; see also Fig. 3E), these results suggest that IFT20 might be implicated in coupling Rab5 to TCRs that have reached early endosomes after their internalization at the cell surface.

We reasoned that if IFT20 is implicated in directing internalized TCRs from $Rab5^+$ endosomes to the next step in the pathway we could expect a block that would lead to a build-up of recycling TCRs within the Rab5 compartment in cells lacking IFT20. To test this possibility, we carried out a colocalization analysis of internalized TCRs with Rab5 in control and IFT20KD cells. An increased colocalization of internalized TCR with Rab5 was detected in IFT20KD cells (Fig. 2C,D). This was paralleled by a decreased colocalization with Rab4 as well as (albeit to a lower extent) with Rab11 (Fig. 2D). Hence, IFT20 promotes the transit of internalized TCRs from early to recycling endosomes.

IFT20 is required for recycling of TCR and TfR, but not of CXCR4

The association of IFT20 with Rabs that are general regulators of endosome recycling raises the question of whether IFT20 selectively controls TCR recycling within these pathways. To address this issue, we first tracked the fate of internalized receptors in recycling experiments. In addition to the TCR, which associates with $Rab11^+$ as well as $Rab4^+$ endosomes (Liu et al., 2000; Kumar et al., 2011), we analyzed two other recycling receptors; the chemokine receptor CXCR4, which localizes in $Rab11^+$ endosomes (Kumar et al., 2011), and the TfR, which recycles through both the Rab4- and the Rab11-dependent routes (Mayle et al., 2012). TCR, TfR and CXCR4 internalization was induced in control and IFT20KD cells using specific antibodies. Internalized receptors were then allowed to recycle to the cell surface, where they were tracked by flow cytometry using fluorochrome-labeled secondary antibodies. Internalization of none of the three receptors was affected by IFT20 deficiency (supplementary material Fig. S1C). IFT20KD resulted in a severe impairment in both TCR and TfR recycling. By contrast, CXCR4 recycling was unaffected (Fig. 3A). Similar results were obtained in a time-course analysis of the recovery of surface receptor following its downregulation by pharmacological stimulation [with the phorbol ester phorbol 12,13-dibutyrate (PDBu) for the TCR] or stimulation with the specific ligand (CXCL12 for CXCR4) (Fig. 3B). The defect in TfR recycling in IFT20KD cells was confirmed in pulse-chase experiments using fluorochrome-labeled holotransferrin (Fig. 3B). As a complementary approach, cells were treated with receptor-specific antibodies and the internalized receptors were visualized by confocal microscopy. Imaging of the internalized receptors showed that IFT20KD resulted in an increase in the number of endosomes containing

Journal of Cell Science (2014) 127, 1924–1937 doi:10.1242/jcs.139337

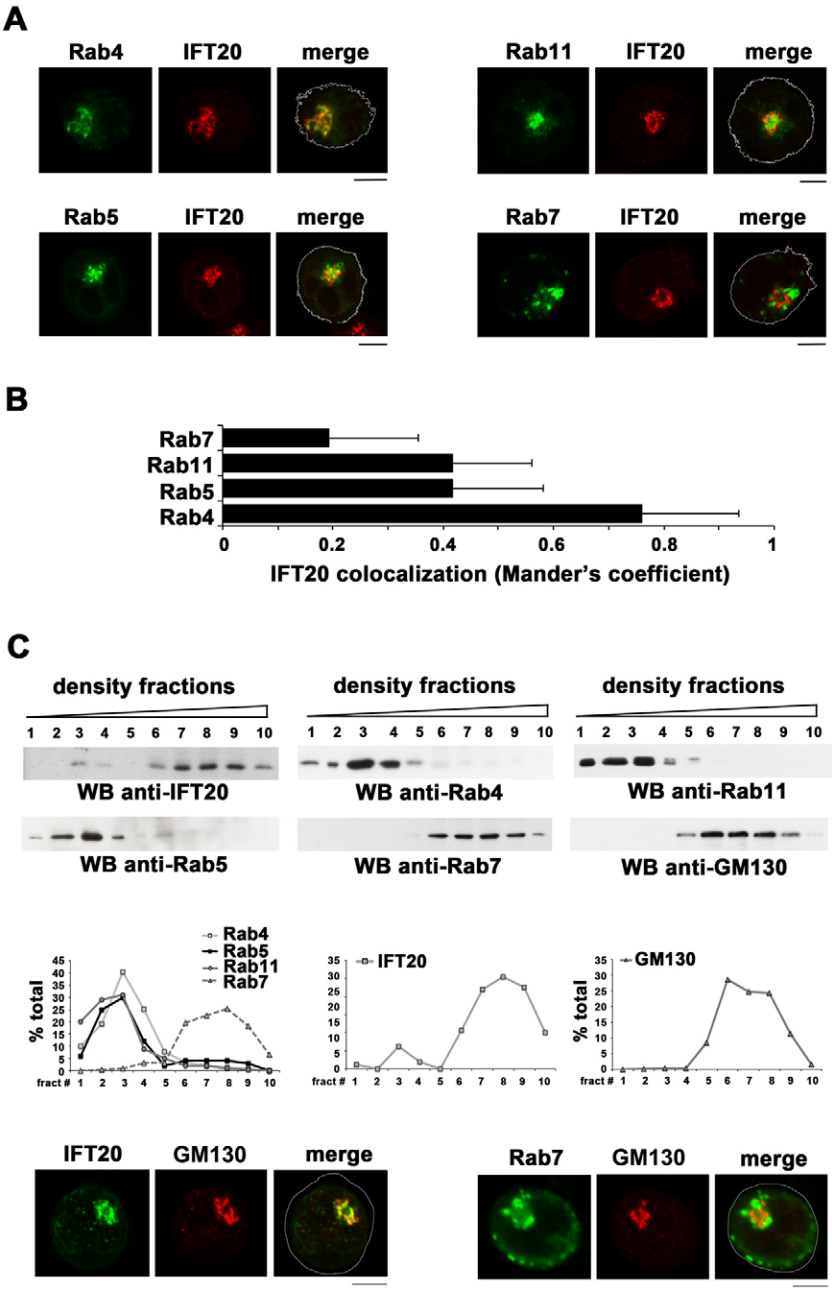

Fig. 1. IFT20 associates with Rab4$^+$, Rab5$^+$ and Rab11$^+$ endosomes. (A) Immunofluorescence analysis of IFT20 in Jurkat cells transiently transfected with constructs encoding GFP-tagged Rab4, Rab5, Rab11 and Rab7. Median optical sections are shown. (B) Quantification (using Mander's coefficient) of the weighted colocalization of IFT20 with the different GFP$^+$ compartments in the GFP-tagged Rab transfectants (mean±s.d.; ≥20 cells/marker; $n \geq 3$). (C) Representative western blot (WB) analysis of Jurkat cell membranes fractionated on 10–30% iodixanol gradients. Immunoreactive bands were quantified using ImageJ and were plotted as specific protein in each fraction vs total specific protein ($n \geq 3$). An immunofluorescence analysis of GM130 in Jurkat cells transfected with GFP-tagged IFT20- or Rab7-encoding constructs is shown below. Scale bars: 5 μm.

internalized TCR or TfR, but not CXCR4 (Fig. 3C). Taken together with the defect in TCR and TfR recycling in IFT20KD T cells that was identified by flow cytometry, these findings further support the notion that TCR and TfR recycling is impaired in IFT20KD T cells, resulting in intracellular accumulation of these receptors. The selective defect in TCR and TfR recycling was confirmed by using flow cytometric analyses of normal T cells transiently knocked down for IFT20 expression (Fig. 3D). Restoration of IFT20 expression in IFT20KD cells resulted in the rescue of the TCR and TfR recycling defects (Fig. 4A,B), confirming that these are caused by the loss of IFT20. Consistent with the implication of IFT20 in TfR recycling, similar to the TCR, this receptor, but not CXCR4, was found to co-precipitate with IFT20 (Fig. 3E). Hence, while interacting with Rabs that are general regulators of endosome recycling, IFT20 controls the recycling of specific receptors.

Rab4, Rab5 and Rab11 polarize to the immune synapse in an IFT20-dependent manner

The association of IFT20 with Rab4 and Rab11 suggests that the immune synapse, where the endosome-associated TCR pool undergoes polarized recycling (Das et al., 2004), might be a target of the recycling pathways that are regulated by IFT20. To address this issue, the localization of Rab4 and Rab11, as well as that of Rab7 as a recycling-unrelated control, was investigated in antigen-specific conjugates of Jurkat cells with Staphylococcal enterotoxin E (SEE)-loaded Raji cells, in which the latter were used as APCs. Rab4 and Rab11, but not Rab7, effectively polarized to the immune synapse, together with IFT20 (Fig. 5A). The polarization of Rab4 and Rab11 to the immune synapse was impaired in IFT20KD cells (Fig. 5A), despite the fact that the centrosome polarizes normally in these cells (Finetti et al., 2009; supplementary material Fig. S2A). By contrast, IFT20 deficiency

Journal of Cell Science (2014) 127, 1924–1937 doi:10.1242/jcs.139337

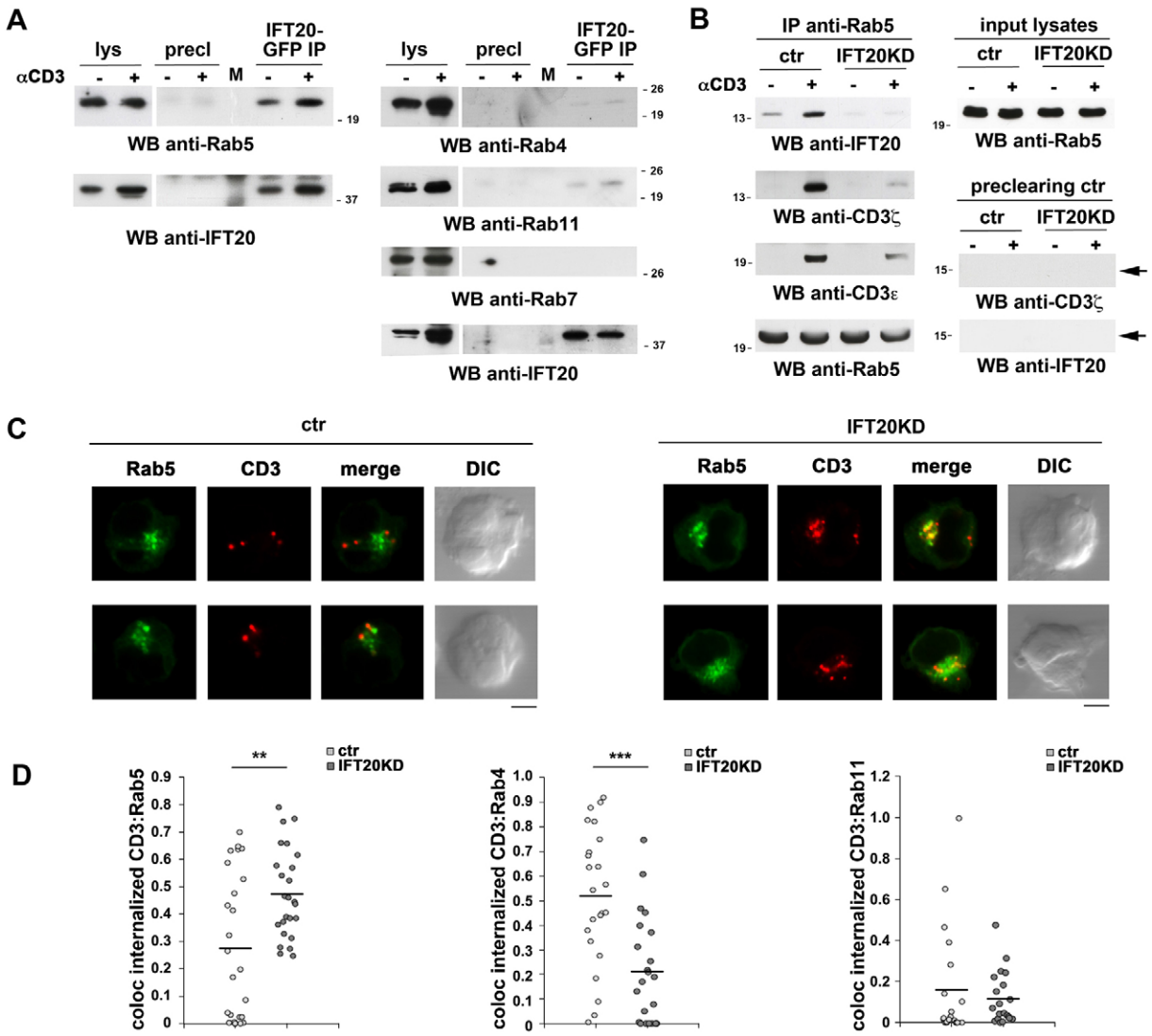

Fig. 2. IFT20 interacts with Rab5 and is required for TCR trafficking from early endosomes. (A) Western blot (WB) analysis with the indicated anti-Rab antibodies of GFP-specific immunoprecipitates from lysates of a stable Jurkat transfectant expressing GFP-tagged IFT20, that was either unstimulated or activated for 10 min by TCR cross-linking (n=3). Preclearing controls (proteins that bound to Protein-A–Sepharose before the addition of primary antibody; precl) are included in each blot. Input lysates (lys) are shown. M, lane containing molecular-mass marker. (B) Immunoblot analysis of Rab5-specific immunoprecipitates from lysates of stable control (ctr) or IFT20KD Jurkat cells, either unstimulated or activated for 10 min by TCR cross-linking (n=3). Input lysates are shown. The arrow in the preclearing control blot shows the migration of CD3ζ or IFT20 in lysates run on the same gel. (C) Immunofluorescence analysis of internalized TCR in control or IFT20KD Jurkat cells transfected with GFP-tagged Rab5. The analysis was carried out at 24 h post-transfection (n=3). Representative images are shown. DIC, differential interference contrast. Scale bars: 5 μm. (D) Quantification (using Mander's coefficient) of the weighted colocalization of the $CD3^+$ vesicles with the GFP^+ compartments in medial confocal sections of control or IFT20KD Jurkat cells transiently transfected with GFP-tagged Rab5, Rab4 or Rab11 (mean±s.d.; ≥25 cells/line; n=3). $^{**}P<0.01$, $^{***}P<0.001$.

did not affect the low levels of Rab7 polarization to the immune synapse (Fig. 5A). Hence, both fast- and slow-recycling endosomes polarize to the immune synapse in an IFT20-dependent manner. Rab5 also polarized to the immune synapse. Similar to the recycling Rabs, this process was dependent on IFT20 (Fig. 5A).

To verify that the polarization of the recycling endosomes was coupled to the delivery of their receptor cargo to the immune-synapse membrane, we tracked the fate of internalized TCR, TfR and CXCR4 in antigen-specific conjugates of control and IFT20KD cells. Receptor internalization was induced by incubating the cells with specific antibodies. Cells were then mixed with SEE-loaded APCs and the conjugates were stained with secondary antibodies without prior permeabilization. Under these conditions, only the receptors that had recycled could be visualized. Consistent with their polarized recycling, TCR and TfR concentrated at the immune synapse in control cells (Fig. 5B). The same applied to CXCR4, which had previously been shown to cluster to the immune synapse (Pérez-Martínez et al., 2010), but for which polarized recycling had not previously been demonstrated (Fig. 5B). Both the TCR and the TfR failed to recycle to the immune synapse in IFT20KD cells, whereas CXCR4 recycling was unaffected (Fig. 5B). Similar results were obtained by using normal peripheral T cells that were transiently knocked down for IFT20 and conjugated to Staphylococcal enterotoxin B (SEB)-loaded APCs (Fig. 5C). The defects in

Journal of Cell Science (2014) 127, 1924–1937 doi:10.1242/jcs.139337

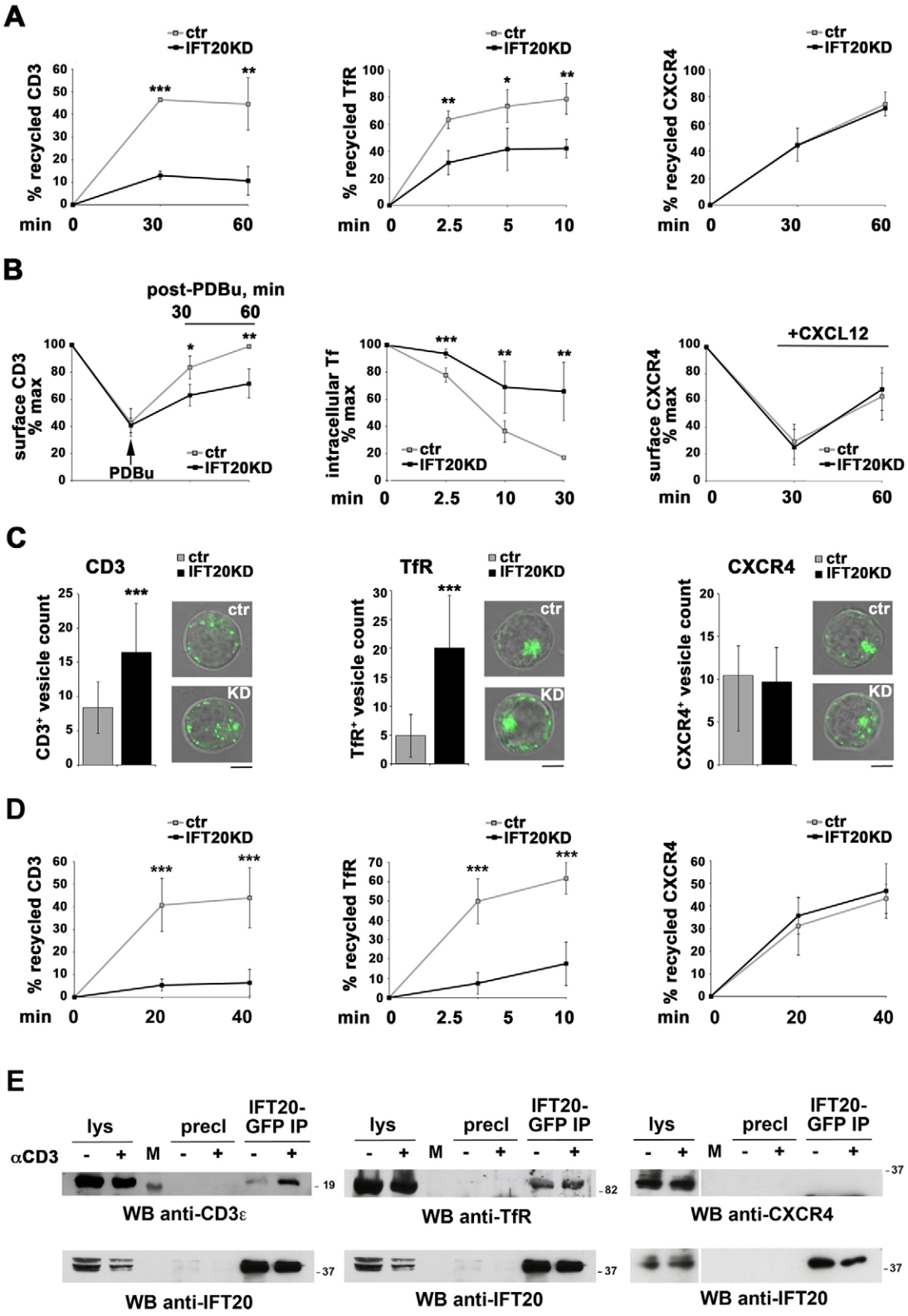

Fig. 3. See next page for legend.

polarized TCR and TfR recycling in IFT20KD cells were rescued by the restoration of IFT20 expression, confirming the causal role of IFT20 in this process (Fig. 4C). Recycling experiments that were performed on permeabilized antigen-specific conjugates showed that, in agreement with the impaired ability of the recycling Rabs to polarize to the immune synapse in IFT20-deficient cells, endosomes containing internalized TCR and TfR were polarized in control cells, but not in IFT20KD cells (supplementary material Fig. S2B). Hence, IFT20 controls the polarization and recycling of a specific subset of receptors to the immune-synapse membrane.

Fig. 3. IFT20 is required for TCR and TfR, but not CXCR4, recycling. (A) Flow cytometric analysis of TCR, TfR and CXCR4 recycling in control (ctr) and IFT20KD Jurkat cells. Data are presented as the percentage of internalized receptors that have recycled to the cell surface and show the mean±s.d. of duplicate samples from three independent experiments. (B) Flow cytometric analysis of receptor recycling in control and IFT20KD Jurkat cells. Left, cells were treated with PDBu to block TCR recycling, then washed and incubated at 37°C to allow recycling to resume. The relative levels of surface TCR were measured before (100%) and after PDBu treatment, and at the indicated times after PDBu removal. Middle, cells were incubated with fluorochrome-labeled holotransferrin and washed to remove excess ligand (0 min). Unlabeled holotransferrin was then added and the samples were incubated at 37°C for the indicated times. Recycling was measured as the relative loss of fluorochrome-labeled transferrin (the transferrin-associated fluorescence at time 0 taken as 100%). Right, CXCR4 recycling was induced by incubation with CXCL12. The relative levels of CXCR4 were measured before CXCL12 addition (100%) and at each time point thereafter. The data show the means±s.d. of duplicate samples from three independent experiments. (C) Counts of vesicles containing internalized CD3, TfR or CXCR4 in control and IFT20KD Jurkat cells. The data are presented as the number of labeled vesicles in medial confocal sections (mean±s.d.; ≥20 cells/receptor). Representative images from four independent experiments are shown. Scale bars: 5 μm. (D) Flow cytometric analysis of TCR, TfR and CXCR4 recycling in normal peripheral T cells (SEB-expanded for the TfR experiments) transiently transfected with empty vector or the same vector encoding IFT20-specific siRNAs (~72% KD). A GFP-encoding construct was included in each transfection as a control. Recycling was analyzed at 24 h post-transfection, gating on GFP^+ live cells. The data, which for each time-point refer to duplicate samples from three independent experiments, are presented as the percentage of the internalized receptors that had recycled to the cell surface (mean±s.d.). $^*P<0.05$, $^{**}P<0.01$, $^{***}P<0.001$. (E) Western blot (WB) analysis with anti-CD3ε, -TfR or -CXCR4 antibodies of GFP-specific immunoprecipitates from lysates of a stable Jurkat transfectant expressing GFP-tagged IFT20, either unstimulated or activated for 10 min by TCR cross-linking ($n\geq2$). Preclearing controls (proteins bound to Protein-A–Sepharose before the addition of primary antibody; precl) are included in each blot. Input lysates (lys) are shown. M, lane containing molecular-mass marker. Note that the same membrane was used for the anti-CD3ε and anti-TfR blots.

IFT57 and IFT52 cooperate with IFT20 to control constitutive and polarized TCR and TfR recycling

We have previously shown that IFT20 forms a complex with IFT57 and IFT88, the formation of which is enhanced in response to TCR stimulation and requires IFT20 expression (Finetti et al., 2009). This suggests that IFT20 might cooperate with other components of the IFT system to control endosome recycling as well as the formation of the immune synapse. To address this issue, we first measured the expression of all the IFT polypeptides in Jurkat cells, using the ciliated HEK293 cells as a control (Gerdes et al., 2007). Quantitative real-time (RT)-PCR analysis showed that all components of the IFT system are expressed in T cells (supplementary material Fig. S3A).

To understand whether IFT20-dependent recycling requires the interplay of IFT20 with other IFT components, we initially focused on IFT57, a component of the IFT-B complex. In addition to participating in the formation of canonical IFT particles in ciliated cells, IFT57 associates with IFT20 and IFT52 on cargo vesicles in non-ciliated secondary retinal neurons (Sedmak and Wolfrum, 2010) and interacts with IFT20 in T cells (Finetti et al., 2009). Immunofluorescence analysis of IFT57 in Jurkat T cell transfectants expressing the Rab–GFP fusions revealed a vesicular pattern that overlapped, albeit to a limited extent, with Rab4, Rab5 and Rab11 (supplementary material Fig. S3B). Interestingly, although a strong colocalization of IFT57 with the centrosome was observed, as assessed by γ-tubulin co-staining, IFT57 did not colocalize with the Golgi (supplementary material Fig. S3B), at variance with IFT20. These results indicate that the vesicular localization of IFT57 might be restricted to post-Golgi compartments.

To address the potential implication of IFT57 in receptor recycling, IFT57 expression was knocked down in Jurkat cells by RNA interference (RNAi, ~40% KD). The fate of internalized TCR, TfR and CXCR4 was assessed in recycling experiments. Flow cytometric analysis showed that, similar to IFT20KD, IFT57 deficiency resulted in a recycling defect that affected selectively TCR and TfR, but not CXCR4 (Fig. 6A). The recycling defect in IFT57KD cells was confirmed by imaging internalized receptors, which revealed an endosomal accumulation of TCR and TfR, but not of CXCR4 (Fig. 6A). Interestingly, knockdown of IFT57 in IFT20KD cells (~50% IFT57 KD) did not result in a more severe recycling defect (supplementary material Fig. S4A,B), indicating that IFT57 participates in the regulation of TCR and TfR recycling in the same pathway as IFT20.

Immunofluorescence analysis of IFT57 in antigen-specific conjugates showed that IFT57 polarizes to the immune synapse together with Rab4, Rab11 and Rab5 (supplementary material Fig. S3C). To assess whether IFT57 is implicated in membrane trafficking during immune synapse formation, the impact of IFT57KD on polarized recycling was addressed. IFT57 deficiency resulted in impaired TCR and TfR polarization to the immune synapse (Fig. 7A). Consistent with this defect, the assembly of a functional immune synapse was prevented in IFT57KD cells, as assessed by measuring the proportion of conjugates harboring phosphotyrosine staining at the APC contact (Fig. 7B). Remarkably, IFT20 failed to polarize to the immune synapse in the absence of IFT57 (Fig. 7B). Taken together with our finding that IFT57 is recruited to the immune synapse in an IFT20-dependent fashion (Finetti et al., 2009), the data suggest that IFT20 and IFT57 act together during the assembly of the immune synapse. In support of this notion, IFT57 depletion in IFT20KD cells did not exacerbate the immune synapse defect observed in cells deficient for the individual proteins (supplementary material Fig. S4E).

The analysis of receptor recycling was extended to cells knocked down for IFT52. Although no antibodies suitable for imaging IFT52 in our cells were available, the efficiency of RNAi (~70% IFT52 KD) at the mRNA level was sufficiently high to carry out the analysis. Moreover, as in the IFT57 KD experiments, a GFP reporter was included to track transfected cells. Similar to IFT20KD or IFT57KD, IFT52 deficiency resulted in impaired TCR, but not CXCR4, recycling (Fig. 6B). A defect in TfR recycling was also observed in IFT52KD cells (Fig. 6B), albeit significantly milder when compared with cells that were deficient for IFT20 or IFT57. IFT52 deficiency also resulted in impaired TCR polarization to the immune synapse and impaired phosphotyrosine signaling (Fig. 7A,B). Interestingly, a significant defect was observed when TfR polarization was analyzed (Fig. 7A), notwithstanding the mild impact of IFT52 deficiency on TfR recycling (Fig. 6B). Similar to results obtained in IFT57KD cells, IFT20 failed to polarize to the immune synapse in the absence of IFT52 (Fig. 7B). These defects were not exacerbated in T cells lacking both IFT20 and IFT52 (~60% IFT52 KD) (supplementary material Fig. S4C–E). Hence, multiple components of the IFT system function in the same pathway of endosome recycling, and they act in concert to control polarized TCR and TfR recycling, as well as tyrosine kinase signaling, at the immune synapse.

Journal of Cell Science (2014) 127, 1924–1937 doi:10.1242/jcs.139337

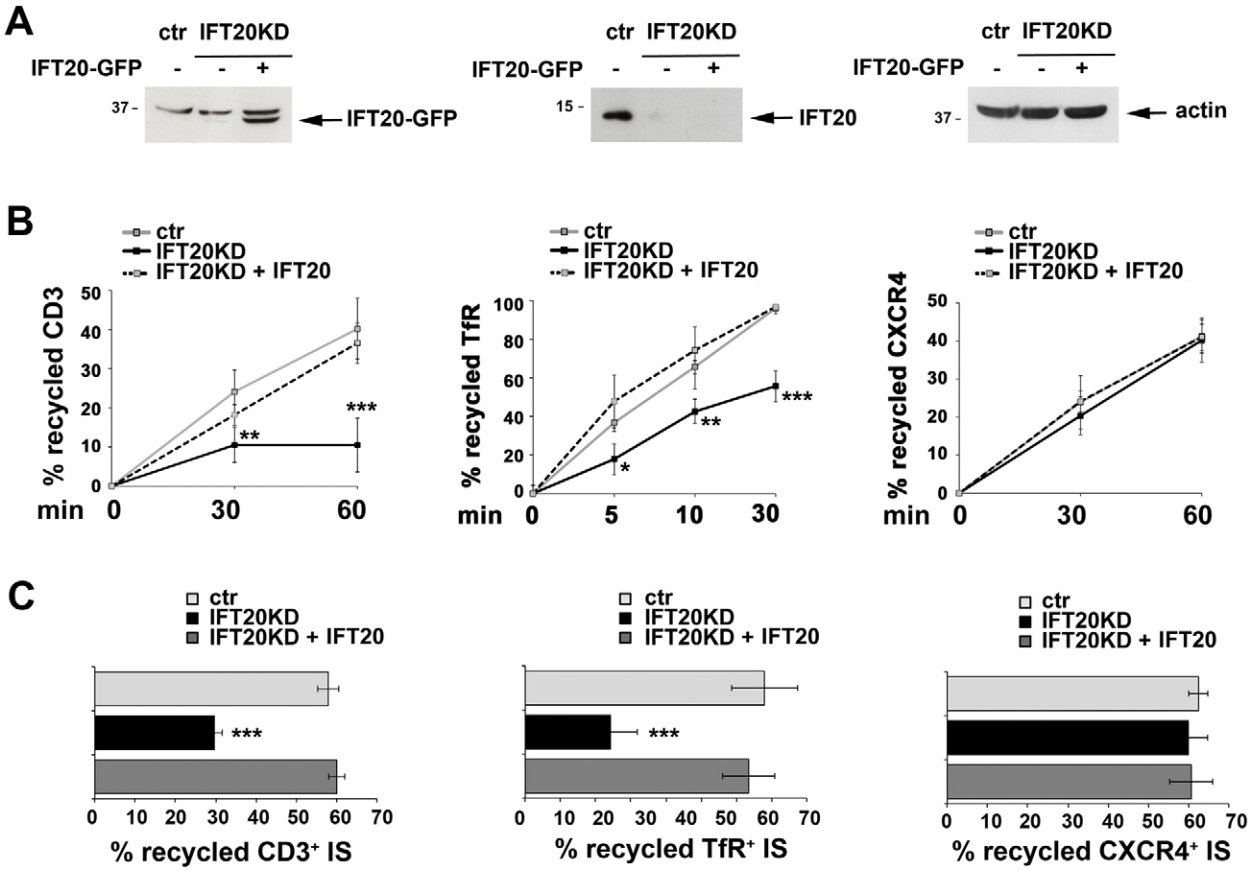

Fig. 4. IFT20 expression in IFT20KD T cells rescues the recycling defects. (A) Representative IFT20 blot on lysates from control (ctr) and IFT20KD cells, transfected with either empty vector (−) or with the IFT20-GFP construct (+), shows that, under these conditions, IFT20–GFP was detectable at significant levels in IFT20KD cells, notwithstanding the presence of interfering RNAs (relative IFT20 expression: ctr, 100%; IFT20KD, 9%; IFT20KD+IFT20–GFP, 158%), possibly due either to the robust transcription driven by the CMV enhancer or to a higher stability of the hybrid transcript. Note that the left panel shows a shorter exposure of the anti-IFT20 blot compared with that shown for endogenous IFT20 in the middle panel, to discriminate the specific signal from the nonspecific signal present in all lanes. (B) Flow cytometric analysis of TCR, TfR and CXCR4 recycling in control and IFT20KD Jurkat cells, the latter either with or without transient transfection with a construct encoding GFP-tagged IFT20. The data are presented as the percentage of the internalized receptors that had recycled to the cell surface and show the mean±s.d. of duplicate samples from three independent experiments. (C) Quantification of the percentage of conjugates harboring recycled TCR, TfR or CXCR4 at the immune synapse (IS) in control and IFT20KD Jurkat cells, the latter either with or without transient transfection with a construct encoding GFP-tagged IFT20 (relative IFT20 expression as in A). Data show the mean±s.d.; $n=3$. *$P<0.05$, **$P<0.01$, ***$P<0.001$.

DISCUSSION

The TCR uses both the slow- and the fast-recycling routes to return to the cell surface, as indicated by its association with Rab11$^+$ and Rab4$^+$ endosomes (Liu et al., 2000; Kumar et al., 2011). How specificity is achieved within these widely used recycling pathways remains to be established. Here, we show that IFT20 colocalizes with Rab4 and Rab11, indicating that IFT20 participates in both routes of TCR recycling. IFT20 also colocalizes with Rab5, suggesting that it might sort internalized TCRs at the level of early endosomes. This notion is strongly supported by the finding that Rab5 and CD3ζ form a complex that includes and requires IFT20. Moreover, recycling TCRs accumulate in Rab5$^+$ endosomes in the absence of IFT20, with a concomitant reduction in Rab4$^+$ and, to a lesser extent, in Rab11$^+$ endosomes. Imaging of Rab4, Rab5 and Rab11 on endosomal membranes of epithelial cells has revealed the existence of three populations, one of which contains Rab5, whereas the others display distinct domains enriched in Rab5 and Rab4, and Rab4 and Rab11, respectively (Sönnichsen et al., 2000). This suggests the possibility that, following its association with the TCR and Rab5, IFT20 might assist the recruitment of Rab4 and Rab11 to distinct membrane domains within early endosomes, promoting the formation of Rab4$^+$ and Rab11$^+$ vesicles containing TCR cargo. The fact that IFT20 shows a significant colocalization with Rab4, as well as with Rab11, but a very limited ability to interact with these Rabs, suggests that it might remain bound to the TCR as this receptor trafficks through the recycling endosomes. An alternative possibility is suggested by the fact that the endosomal localization and recycling-related function of IFT20 is recapitulated by the Arp2/3 adaptor complex WASH, which regulates the trafficking of endosomes by assisting their interaction with microtubules (Gomez and Billadeau, 2009). Although the ability of the IFT particles to interact with microtubule motors (Pedersen and Rosenbaum, 2008) might suggest a similar scenario for IFT20-dependent recycling in T cells, we have not detected an interaction of IFT20 with either the kinesin Kif3A or with dynein in co-immunoprecipitation experiments (A.O., data not shown), which makes this possibility unlikely.

The function of IFT20 as a device to mark recycling endosomes containing specific receptors is supported by the finding that, besides impairing TCR recycling, IFT20 deficiency

Journal of Cell Science (2014) 127, 1924–1937 doi:10.1242/jcs.139337

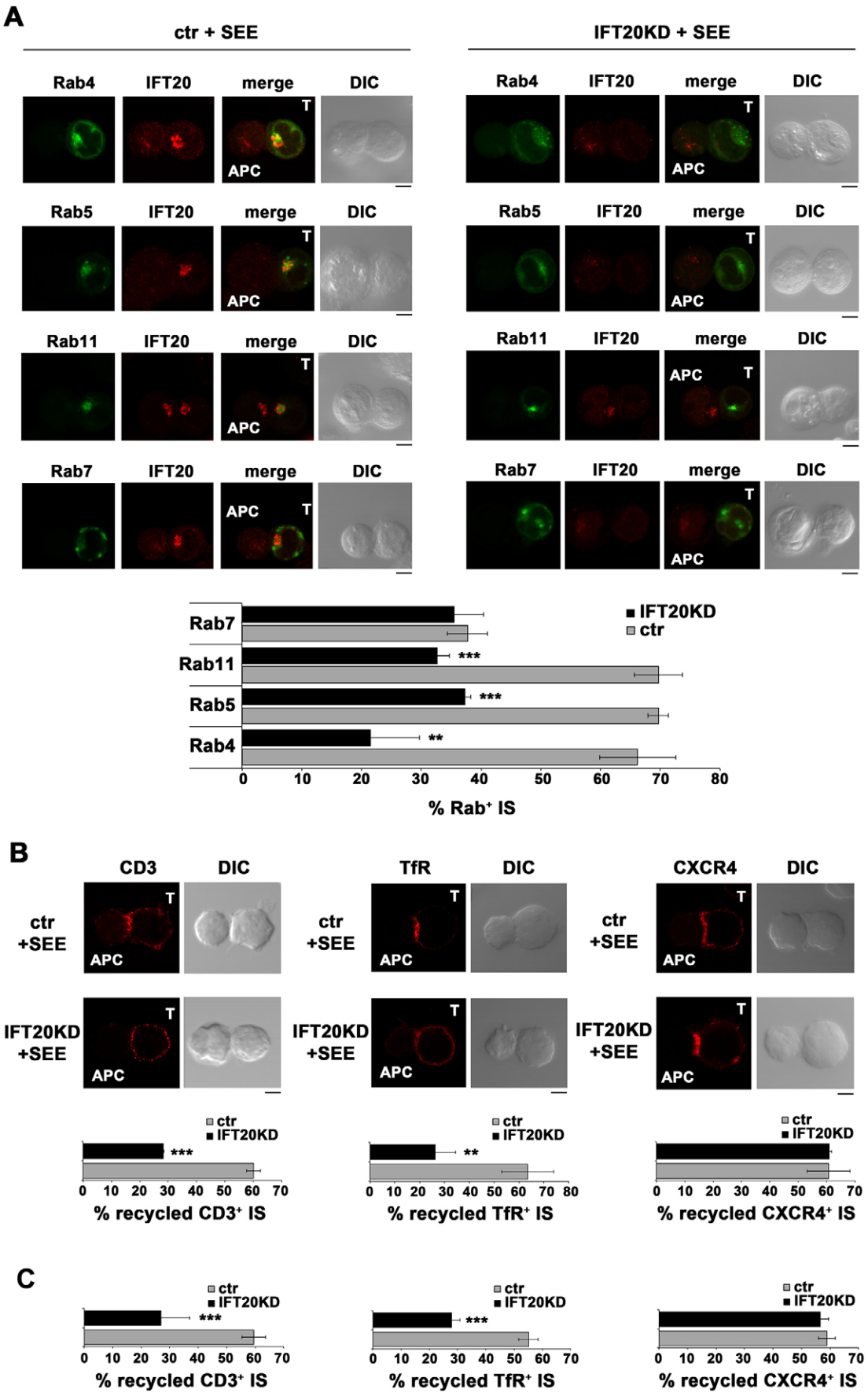

Fig. 5. See next page for legend.

Journal of Cell Science (2014) 127, 1924–1937 doi:10.1242/jcs.139337

Fig. 5. IFT20 is required for Rab polarization and TCR and TfR delivery to the immune synapse. (A) Immunofluorescence analysis of GFP-tagged Rab4, Rab5, Rab11 and Rab7 (green) in conjugates of control (ctr) or IFT20KD Jurkat cells and SEE-pulsed Raji cells (APC). Cells were co-stained with anti-IFT20 antibodies (red). Quantification of the percentage of conjugates with Rab polarization at the immune synapse (IS) are shown below. Data show the mean±s.d., $n>3$. DIC, differential interference contrast. (B) Immunofluorescence analysis of recycled TCR, TfR and CXCR4 in conjugates of control or IFT20KD Jurkat cells and SEE-pulsed Raji cells (APC). Quantification of the percentage of conjugates harboring recycled TCR, TfR or CXCR4 at the immune synapse are shown below (data show the mean±s.d.). Median optical sections are shown. Measurements were taken on ≥300 conjugates from three independent experiments. Scale bars: 5 μm. (C) Quantification of the percentage of conjugates harboring recycled TCR, TfR or CXCR4 at the immune synapse (measured as in B) using SEB-expanded normal T cells transiently knocked down for IFT20 expression (~72% KD) and SEB-pulsed Raji cells ($n=3$). Data show the mean±s.d. $^{**}P<0.01$; $^{***}P<0.001$.

results in impaired recycling of the TfR, but not of CXCR4 [notwithstanding the fact that CXCR4 also uses the Rab11-dependent pathway to recycle to the cell surface (Kumar et al., 2011)], which suggests that the TCR and CXCR4 might associate with distinct subpopulations of $Rab11^+$ endosomes. Taken together with the observation that the TfR and the glucose transporter GLUT4 (also known as SLC2A4) are sorted from early endosomes to two independent sets of $Rab4^+$ vesicles (Lim et al., 2001), these results indicate that multiple recycling pathways that are tailored for specific receptors are operational within the general recycling pathways orchestrated by Rab4 and Rab11, and that IFT20 (and, at a more general level, the IFT system) is a central participant in the orchestration of these specific pathways. Although TfR recycling proceeds through a default pathway that does not require a sorting signal (Maxfield and McGraw, 2004), in T cells the TfR is constitutively associated with CD3ζ (Salmerón et al., 1995). This shared component of the TCR or CD3 complex and the TfR might account for the ability of this receptor to interact with IFT20 as well as for the TfR recycling defect in IFT20KD cells. This notion is supported by the fact that TfR recycling in B cells, which lack CD3ζ, is not affected by IFT20 deficiency (L. P., data not shown). The cytosolic domains of the CD3 components have no homology with known signals of ciliary sorting (Pazour and Bloodgood, 2008) and, indeed, pull-down experiments with GST-tagged IFT20 ruled out a direct interaction of IFT20 with CD3ζ (G. M., data not shown), indicating that specific adaptors might be responsible for IFT20 recruitment to endosomes containing these receptors.

The role of IFT20 as a regulator of receptor recycling in T cells extends to the polarized recycling to the immune synapse. Centrosome polarization beneath the contact area with the APC, which occurs following TCR engagement, is not affected by IFT20 deficiency (Finetti et al., 2009), ruling out a role for IFT20 in the initial mobilization of surface TCR to the nascent immune synapse. By contrast, recycling of both the TCR and the TfR to the immune synapse is severely impaired in IFT20KD cells, pinpointing the role of IFT20 to the membrane-trafficking-dependent phase of receptor clustering to the immune synapse. It is noteworthy that $Rab5^+$ endosomes also polarize to the immune synapse in an IFT20-dependent fashion, suggesting that IFT20 might be recruited to endosomes containing TCR complexes that have been engaged and internalized at the immune synapse, and promote their recycling to the same location. Although activated TCRs that are internalized at the immune synapse are ubiquitylated and targeted to lysosomes by the ESCRT-1 complex (Vardhana et al., 2010), it has been proposed that they might undergo recycling before degradation (Das et al., 2004). Moreover, a recent report shows that tyrosine-phosphorylated CD3ζ accumulates in endosomal vesicles that are distinct from lysosomes (Yudushkin and Vale, 2010). Hence, IFT20 might initially promote the polarized recycling of quiescent TCRs to the nascent immune synapse and subsequently assist the recycling of activated internalized TCRs to the immune synapse. It should be emphasized that, notwithstanding the effective translocation of both the centrosome and the Golgi complex towards the APC contact (Finetti et al., 2009), IFT20KD results in a significant defect in Rab5, Rab4 and Rab11 polarization to the immune synapse. This implies that, although IFT20 deficiency does not have a generalized effect on receptor recycling, as shown by the fact that CXCR4 recycling proceeds normally in these cells, IFT20 might be implicated in recycling of other receptors that traffic both through the fast and the slow routes.

The delivery of membrane-associated cargo to the primary cilium is regulated by exocytic pathways that ensure the sorting of ciliary proteins, their polarized transport to the base of the cilium and their delivery into the cilium, as underscored by expanding evidence that traffic regulators, such as Rab11, Rab8 and Rabin8 (the latter of which is also known as RAB3IP), the TRAPPII complex and UNC-119 are implicated in ciliogenesis. Moreover, the cilium itself is emerging as a secretory device, as demonstrated by its ability to secrete bioactive ectosomes (Wood et al., 2013). Both the IFT particles and the BBSome (a multiprotein complex associated with the basal body and the primary cilium) participate as central players in the ciliary targeting of membrane proteins (Finetti and Baldari, 2013) and, moreover, the IFT system has been recently shown to participate in the first steps of autophagosome formation by assisting the localization of autophagy-related proteins at the base of the cilium (Pampliega et al., 2013). The function of the IFT system as a device for directional vesicular trafficking to a specialized membrane patch that eventually evolved into a cilium, was initially hypothesized based on bioinformatic analyses, which revealed structural homologies between IFT polypeptides and components of vesicle coats (Jékely and Arendt, 2006). These similarities extend to the components of the BBSome, which actually polymerize a coat in the presence of the Arf-like GTPase ARL6 (also known as BBS3) (Jin et al., 2010). Although there is no experimental evidence that IFT proteins can act as coatomers, the original trafficking function of the IFT system is supported by the finding that two IFT proteins, IFT22 and IFT27, are Rab-like GTPases (Schafer et al., 2006; Qin et al., 2007). Moreover, elipsa (also known as IFT54) has been shown to interact genetically with IFT20 and the Rab5 effector, Rabaptin5 (Omori et al., 2008), with the caveat that the IFT20 interaction with Rabaptin5 was not confirmed in mammalian cells (Follit et al., 2009).

An important issue raised by the proto-coatomer hypothesis is whether the IFT system serves a trafficking-related function independently of cilia and whether its components cooperate in this function, as they do in IFT particles. Two IFT-B components, IFT52 and IFT57, have been shown to colocalize in vesicle-like structures in secondary retinal neurons (Sedmak and Wolfrum, 2010), suggesting that IFT complexes might be associated with membrane trafficking in non-ciliated cells. Our identification of IFT20 in TCR recycling in the non-ciliated T cell (Finetti et al., 2009) has provided experimental evidence in favor of this notion, which is further supported by the results presented here that document an interplay of IFT20 with several recycling Rabs, in

Journal of Cell Science (2014) 127, 1924–1937 doi:10.1242/jcs.139337

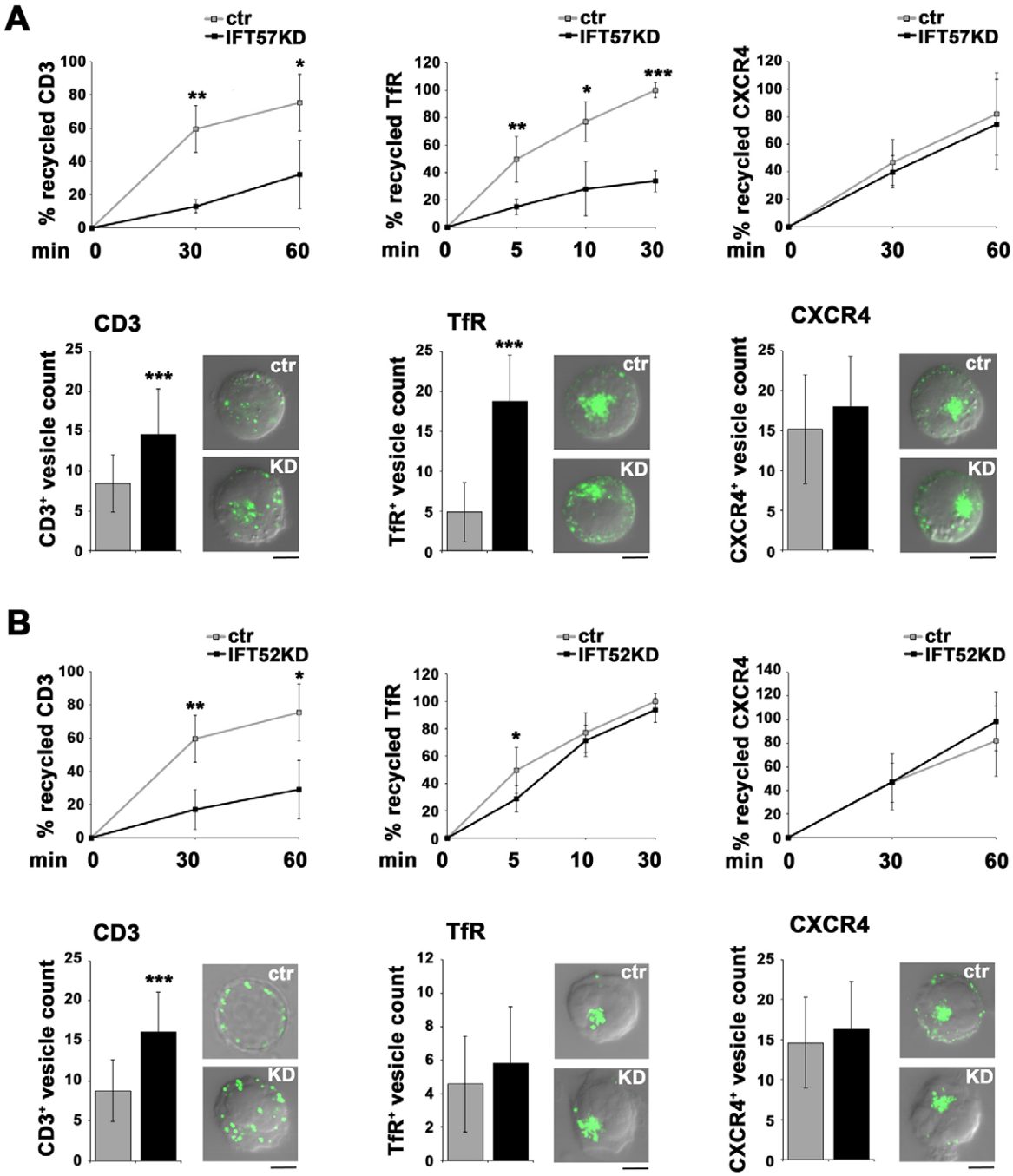

Fig. 6. IFT57 and IFT52 participate in TCR and TfR recycling. (A,B) Upper panels, flow cytometric analysis of TCR, TfR and CXCR4 recycling in Jurkat cells knocked down for IFT57 (A) or IFT52 (B) expression by RNAi. A GFP-encoding construct was included in each transfection as a control (ctr). Recycling was analyzed at 24 h post-transfection, gating on GFP$^+$ live cells. The data are presented as the percentage of the internalized receptors that recycled to the cell surface and show the mean±s.d. for duplicate samples from three independent experiments. (A,B) Lower panels, counts of vesicles containing internalized CD3, TfR or CXCR4 in Jurkat cells knocked down for IFT57 (A) or IFT52 (B) expression. Cells were processed and analyzed as in Fig. 3C (≥25 cells/receptor). Representative images from three independent experiments are shown. Scale bars: 5 µm. Data show the mean±s.d. *P<0.05, **P<0.01, ***P<0.001.

conjunction with other IFT polypeptides. Indeed, not only are IFT52 and IFT57 required for constitutive and polarized TCR recycling, similar to IFT20, but they appear to participate in the same pathway, as indicated by the failure of IFT52 or IFT57 depletion to exacerbate the recycling defects observed in IFT20KD cells. Moreover, we reported previously that IFT20KD resulted in a failure of IFT57 to polarize to the immune synapse (Finetti et al., 2009) and we now show that, reciprocally, IFT20 recruitment to the immune synapse is impaired in IFT52- or IFT57-deficient cells. These results indicate that IFT20, IFT52 and IFT57 act together within the same pathway to control TCR recycling. Of note, as opposed to its polarized recycling to the immune synapse that, similar to that of the TCR, appears to be regulated by the concerted action of IFT20, IFT57 and IFT52, constitutive TfR recycling is affected only to a minor extent by IFT52 deficiency. This suggests that

Journal of Cell Science (2014) 127, 1924–1937 doi:10.1242/jcs.139337

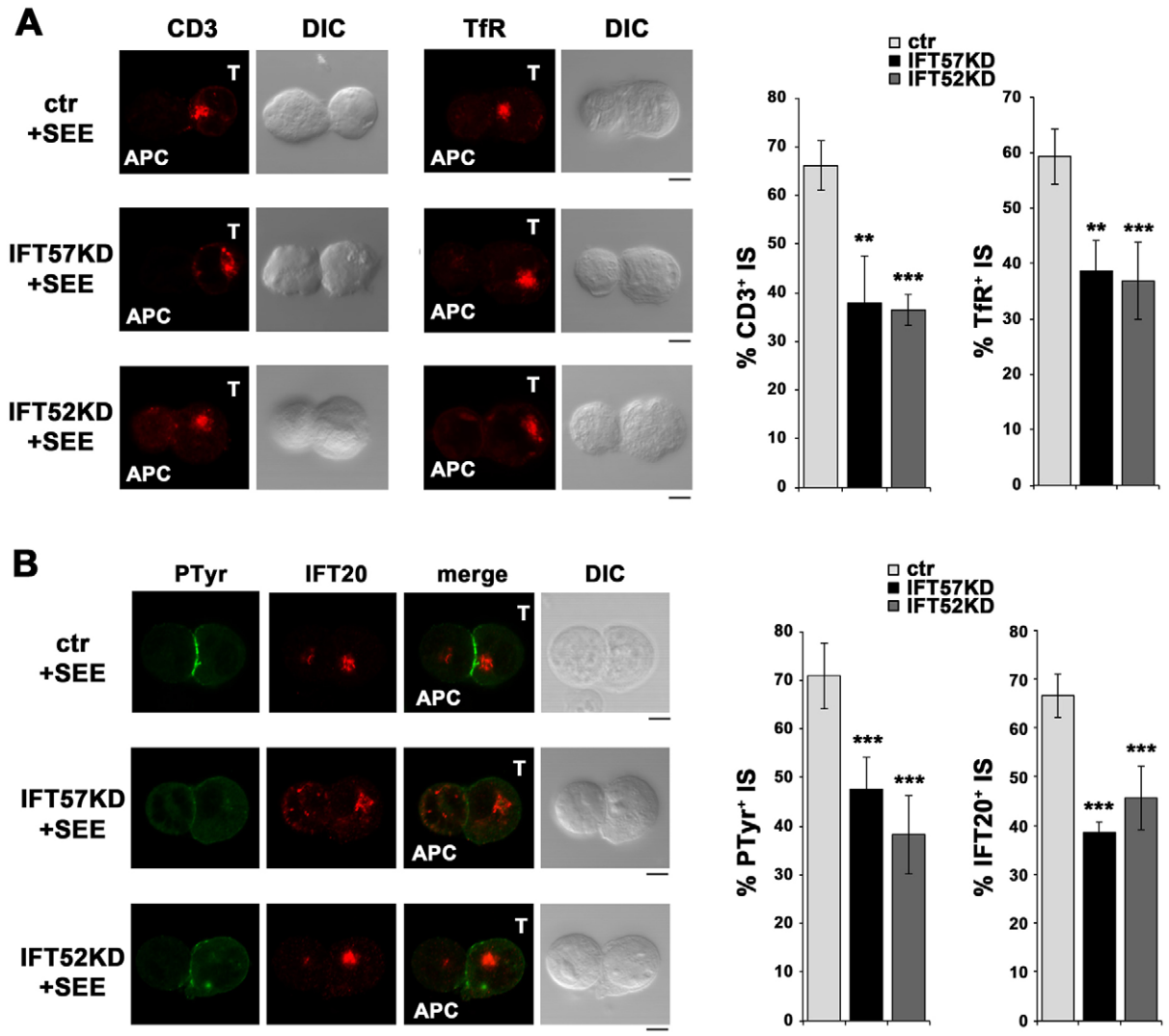

Fig. 7. IFT57 and IFT52 participate in polarized TCR and TfR recycling to the immune synapse. Immunofluorescence analysis of TCR or TfR (A), or phosphotyrosine (PTyr) and IFT20 (B) in conjugates of SEE-pulsed Raji cells (APC) and Jurkat cells knocked down for IFT57 (~40% KD) or IFT52 (~70% KD) expression using IFT-specific siRNAs. RLUC siRNAs were used as a control (ctr). Cells were processed for conjugate formation at 24 h post-transfection. Median optical sections are shown. DIC, differential interference contrast. Scale bars: 5 μm. The histograms show the percentage of conjugates with TCR, TfR or IFT20 polarization, or of conjugates harboring PTyr staining, at the immune synapse (IS). Measurements were taken on ≥300 conjugates from three independent experiments. Data show the mean±s.d. $^{**}P<0.01$, $^{***}P<0.001$.

that IFT57 and IFT52 might participate in different IFT complexes to control TfR recycling in quiescent T cells and during the formation of the immune synapse.

In conclusion, the data presented in this report contribute to our understanding of the mechanisms that regulate TCR trafficking and immune synapse formation, and identify the IFT system as a player in the pathways that control receptor recycling. In addition, our findings demonstrate that the mechanisms that regulate protein targeting to the immune synapse and the primary cilium are shared far beyond the use of the known basic components of the intracellular trafficking machinery, and they highlight an intimate relationship between these two structures.

MATERIALS AND METHODS

Cells, plasmids, transfections, antibodies and reagents

Cells included Jurkat T cells, Raji B cells, HEK293 cells and T cells purified from peripheral blood from healthy donors by Ficoll gradient centrifugation. The latter were either used without further treatment or expanded by using SEB stimulation for 7–10 days (to increase the number of antigen-specific T cells) for the immune synapse experiments and for the TfR recycling experiments, because the TfR is expressed at significant levels only in antigen-experienced T cells (data not shown). Stable control and IFT20KD Jurkat lines were as described previously (Finetti et al., 2009). IFT20KD cells were routinely checked for IFT20 depletion both by immunofluorescence and by immunoblotting (see examples in supplementary material Fig. S1B). A Jurkat cell line stably transfected with the GFP-tagged IFT20 expression construct pJAF2.13 (Follit et al., 2006) was also generated. Human IFT52- and IFT57-specific endoribonuclease-prepared siRNAs (esiRNAs) (Sigma-Aldrich, The Woodlands, TX) and unrelated control *Renilla* luciferase (RLUC) esiRNA (Sigma-Aldrich), or pCMV-EGFP-C3-Rab4a, -EGFP-C3-Rab5a, -EGFP-C1-Rab7 and -EGFP-C3-Rab11 (kindly provided by Peter van der Sluijs and Marino Zerial), were transfected by using electroporation and assays were carried out after 24 h. Immunofluorescence analysis of Rab–GFP transfectants using Rab-specific antibodies showed the same intracellular localization of endogenous and GFP-tagged Rabs (not shown). Freshly isolated and SEB-expanded peripheral T cells were

transiently transfected with the same expression plasmids (or empty vector controls) using the Amaxa nucleofector device (Amaxa Biosystems) and they were analyzed at 24 h post-transfection. For IFT20 rescue experiments, Jurkat cells were transiently transfected with either pJAF2.13 or the GFP-expressing control construct pmaxGFP (Amaxa Biosystems), and were analyzed at 24 h post-transfection.

Polyclonal anti-IFT20 antibodies were as described previously (Pazour et al., 2002). Anti-TfR monoclonal antibody (mAb) (hybridoma OKT9) was generously provided by Andres Alcover, anti-CXCR4 antibodies were provided by James Hoxie (Leukosite, Cambridge, MA), Leukosite and the MRC AIDS Reagent Project. IgG from OKT3 (anti-CD3ε) hybridoma supernatants was purified using Mabtrap (Amersham Biosciences) and titrated by flow cytometry. Anti-phosphotyrosine antibodies were from Upstate Biotechnology (Temecula, CA); anti-Rab7, -Rab11, -CD3ζ and -TfR mAbs, as well as anti-CD3ε polyclonal antibodies (goat) were from Santa Cruz Biotechnology (Santa Cruz, CA); anti-GFP polyclonal and monoclonal antibodies were from Invitrogen (Milan, Italy); anti-GM130, -Rab4 and -Rab5 mAb were from BD Biosciences (San Jose, CA); anti-Rab5 and anti-Rab11 polyclonal antibodies were from Cell Signaling Technology (Boston, MA); anti-Rab4 polyclonal antibodies were from Abcam (Cambridge, UK); anti-actin mAb was from Merck Millipore (Billerica, MA); anti-γ-tubulin mAb was from Sigma-Aldrich; anti-CXCR4 mAb was from Abnova (Taipei, Taiwan). Unlabeled secondary antibodies were from Cappel (ICN Pharmaceuticals, CA) and peroxidase-labeled secondary antibodies were from Amersham Biosciences. Alexa-Fluor-488- and Alexa-Fluor-555-labeled secondary antibodies were from Molecular Probes (Invitrogen), PE-conjugated anti-mouse-Ig was from eBiosciences (San Diego, CA).

SEE and SEB were from Toxin Technology (Sarasota, FL), Cell Tracker Blue was from Molecular Probes (Invitrogen); poly-L-lysine, CXCL12 and PDBu were from Sigma-Aldrich, protein-A–Sepharose (PAS) was from Amersham.

Flow cytometry and immunofluorescence analysis of receptor recycling

Receptor recycling was quantified by flow cytometry, using the same batches of control and IFT20KD cells for the comparative analysis of different receptors. Surface levels of TfR and CXCR4 were comparable between control and IFT20KD Jurkat cells, as assessed by flow cytometry. Of note, this also applied to CD3, at variance with our previous report (Finetti et al., 2009). Nonetheless, consistent with the TCR recycling defect described in our previous report, the proportion of surface versus total CD3 was lower in IFT20KD cells (~60%), suggesting that IFT20KD cells might have upregulated CD3 expression to compensate for the recycling defect and normalize the levels of surface CD3.

The optimal times for maximal internalization and recycling of each receptor were initially determined in time-course experiments (supplementary material Fig. S1C,D). For antibody-dependent recycling, cells were equilibrated for 30 min at 37℃ in RPMI 1640 with 1% BSA, then incubated for 30 min on ice with saturating concentrations of receptor-specific mAb to allow binding. Cells were then washed with cold PBS and shifted to 37℃ for 15 min (TfR) or 60 min (TCR, CXCR4) to allow internalization of receptor–mAb complexes. The cells were acid-stripped to remove residual surface-bound mAb [30 s at room temperature (RT) in 100 mM glycine, 100 mM NaCl, pH 2.5] and then were washed and incubated at 37℃ to allow the recycling of receptor–mAb complexes (in the presence of 1 mg/ml holotransferrin for TfR recycling). Receptor–mAb complexes that had recycled to the cell surface were measured by labeling with fluorochrome-labeled secondary antibody. The data are presented as the percentage of the internalized receptors that have recycled to the cell surface as described (Margadant et al., 2012), calculated using the formula

$$x_t = \frac{MFI_t - MFI_s}{(MFI_{max} - MFI_s) - (MFI_n - MFI_s)} \times 100,$$

where MFI_t is the mean fluorescence intensity at time 't', MFI_s is the MFI after acid-stripping of surface-bound mAb, MFI_{max} is the MFI after incubation on ice with receptor-specific mAb and MFI_n is the MFI after receptor–mAb complexes are internalized.

Alternatively, after the equilibration step, recycling was measured as follows. For TCR recycling, cells were incubated with 1 μM PDBu for 60 min at 37℃ in RPMI plus 1% BSA, then washed and incubated for 30 or 60 min at 37℃. The relative levels of surface TCR were measured before (set to 100%) and immediately after PDBu treatment, and 30 or 60 min after PDBu removal. For TfR recycling, cells were incubated with 15 μg/ml fluorochrome-labeled holotransferrin (Molecular Probes) for 30 min on ice, then washed to remove excess ligand and incubated for 15 min at 37℃. After acid-stripping, 1 mg/ml unlabeled holotransferrin was added (Sigma-Aldrich) and the cells were incubated for 5, 10 or 30 min at 37℃. Recycling was measured as the relative loss of fluorochrome-labeled transferrin. For CXCR4 recycling, cells were incubated with 100 ng/ml CXCL12 for 30 min at 37℃. Subsequently, cells were subjected to acid-stripping and then incubated at 37℃ for 30 or 60 min. Relative CXCR4 levels were measured before CXCL12 addition and at each time-point thereafter. Flow cytometry was carried out using a FACScan flow cytometer (Becton Dickinson, San Jose, CA).

For immunofluorescence analysis of vesicles containing internalized receptors, cells were equilibrated as above and were then incubated with saturating concentrations of receptor-specific mAb at 37℃ for 2 h. Cells were washed to remove excess mAb, allowed to adhere for 15 min on poly-L-lysine-coated wells of diagnostic microscope slides (Erie Scientific Company), fixed in 4% paraformaldehyde for 20 min at RT and permeabilized in PBS plus 0.01% Triton X-100 for 20 min at RT. Internalized receptor–mAb complexes were labeled using fluorochrome-labeled secondary antibody and visualized by using confocal microscopy. The number of vesicles that were positive for each receptor was determined on individual medial confocal sections using ImageJ (the 'analyze particles' function) to identify and count objects, setting 0.005 μm^2 as the lowest limit and excluding the compact pericentrosomal compartment where objects could not be discriminated.

Conjugate formation

Conjugates between T cells and superantigen (SAg)-pulsed Raji B cells (used as APCs) were carried out as described previously (Finetti et al., 2009). SEE was used for Jurkat cells, which express a cognate TCR Vβ, whereas SEB was used for normal T cells, as this SAg covers a wider proportion of the Vβ repertoire compared with SEE.

To analyze recycled TCR, TfR or CXCR4 at the immune synapse, cells were equilibrated as above, then incubated with saturating concentrations of receptor-specific mAb at 37℃ for 2 h. Residual surface-bound mAb was removed by acid-stripping. Cells were then mixed with SEE- or SEB-pulsed Raji cells, incubated for 15 min at 37℃, plated onto poly-L-lysine-coated wells and fixed by immersion in methanol for 10 min at −20℃, or analyzed under non-permeabilizing conditions after paraformaldehyde fixation.

Immunofluorescence microscopy and colocalization analyses

Fixed samples were washed for 5 min in PBS and incubated with primary antibodies overnight at 4℃ or for 1 h at RT. After washing in PBS, samples were incubated for 1 h at RT with Alexa-Fluor-488- and Alexa-Fluor-555-labeled secondary antibodies.

Confocal microscopy was performed by using a Zeiss LSM700 with a 63× objective. The z series of optical sections were performed at 0.5-μm increments. Images were acquired with pinholes opened to obtain 0.8-μm-thick sections. Detectors were set to detect an optimal signal below the saturation limits. Images were processed with Zen 2009 image software (Carl Zeiss, Jena, Germany).

The colocalization analyses were performed on T cells transiently transfected with the GFP-tagged Rab constructs. The quantitative colocalization analysis of IFT20 and GFP protein signals in the Jurkat transfectants expressing the different GFP-tagged Rabs was performed on median optical sections using ImageJ and the JACoP plug-in to determine Manders' coefficient M_1 (Manders et al., 1992), which represents the percentage of IFT20 pixels that overlap GFP–Rab pixels.

Membrane fractionation on iodixanol gradients, and electron microscopy

A total of 50×10^6 control Jurkat T cells (empty vector transfectant) (Finetti et al., 2009) were homogenized by 10 passages through a 26-gauge syringe needle, preceded by Dounce homogenization (10 pestle strokes) in 1 ml of homogenization medium (HM; 0.25 M sucrose, 1 mM EDTA, 10 mM Tris-HCl pH 7.4), in the presence of protease inhibitors. The homogenate was centrifuged at 3000 ***g*** for 5 min at 4℃ to remove nuclei and mitochondria, and the supernatant was centrifuged at 68,000 ***g*** for 1 h at 4℃. The microsomal pellet was fractionated by iodixanol gradient centrifugation (Li and Donowitz, 2008). Briefly, the pellet was resuspended in 1.2 ml of HM, mixed 1:1 with 60% iodixanol (Sigma-Aldrich) in buffer diluent (0.25 M sucrose, 6 mM EDTA, 60 mM Tris-HCl pH 7.4), layered onto a gradient consisting of 1.3 ml of 20% iodixanol and 1.2 ml of 10% iodixanol in HM and centrifuged at 350,000 ***g*** for 3 h at 4℃. Ten fractions were collected from the top of the tube and analyzed by SDS-PAGE (equal volumes of each fraction). Electron microscopy after negative staining with 2% uranyl acetate showed the presence of vesicles in all fractions (not shown).

Activation, immunoprecipitation and immunoblotting

Activation was performed by incubating Jurkat cells (5×10^7 cells/sample for the control and IFT20KD transfectants; 7.5×10^7 cells/sample for the IFT20–GFP transfectant), resuspended in 200 µl RPMI, with saturating concentrations of anti-CD3 mAb (determined by flow cytometry for each OKT3 batch) and 50 µg/ml anti-mouse-IgG antibody for 10 min at 37℃. Cells were pelleted, washed twice in ice-cold PBS and lysed in 0.5% Triton X-100 in 20 mM Tris-HCl (pH 8), 150 mM NaCl in the presence of protease inhibitors (Calbiochem). Postnuclear supernatants (2 mg/sample for the control and IFT20KD transfectants; 3 mg/sample for the IFT20–GFP transfectant) were immunoprecipitated for 2 h using 2 µg of anti-Rab5 (BD Biosciences) or anti-GFP mAb (Life Technologies), and PAS (3 mg/sample), after a preclearing step on PAS (1 h, 3 mg/sample). Under these conditions, no TCR (CD3) pulldown by the activating anti-CD3 mAb was detectable (supplementary material Fig. S1E). All gels included a fraction of the lysates used for the IPs (50 µg/sample). Immunoblotting was performed using peroxidase-labeled secondary antibody and a chemiluminescence detection kit (Pierce, Rockford, IL). Membranes were reprobed with control antibodies after stripping. Blots were scanned and quantified by using ImageJ.

RNA purification and RT-PCR

RNA was extracted from Jurkat and HEK293 cells and reverse transcribed as described previously (Patrussi et al., 2007). RT-PCR was performed in triplicate on each cDNA in 96-well optical PCR plates (Sarstedt AG, Nümbrecht, Germany) as described previously (Capitani et al., 2012). Transcript levels were normalized to those of *HPRT1*, which was used as a housekeeping gene. The primers used to amplify the cDNA fragments corresponding to human transcripts are listed in supplementary material Table S1.

Statistical analysis

Means, standard deviations and Student's *t*-test (unpaired) were calculated by using the Microsoft Excel application. $P<0.05$ was considered as statistically significant.

Acknowledgements

The authors wish to thank Joel Rosenbaum (Yale University, New Haven, CT), Peter van der Sluijs (University Medical Center, Utrecht, The Netherlands), Marino Zerial (Max Planck Institute of Molecular Cell Biology and Genetics, Dresden, Germany), Andres Alcover (Institut Pasteur, Paris, France), Antonella De Matteis (The Telethon Institute of Genetics and Medicine, Naples, Italy) and Cecilia Bucci (University of Salento, Lecce, Italy) for useful discussions and for generously providing key reagents; John Telford (Novartis Vaccines and Diagnostics, Siena, Italy) for advice, David Mercati (Univeristy of Siena, Siena, Italy) for electron microscopy and Sonia Grassini (Univeristy of Siena, Siena, Italy) for technical assistance.

Competing interests

The authors declare no competing interests.

Author contributions

F.F., L.P., G.M., O.M.L., A.O. and C.T.B. designed the experiments and analyzed the data; F.F., L.P., G.M., O.M.L., A.O. and D.G. performed the experiments; G.J.P. provided key reagents; F.F., G.J.P. and C.T.B. wrote the paper.

Funding

The work was supported by a grant from Telethon to C.T.B. [grant number GGP11021]; the support of the National Institutes of Health [grant number GM060992 to G.J.P.] is also acknowledged. Deposited in PMC for release after 12 months.

Supplementary material

Supplementary material available online at
http://jcs.biologists.org/lookup/suppl/doi:10.1242/jcs.139337/-/DC1

References

Baldari, C. T. and Rosenbaum, J. (2010). Intraflagellar transport: it's not just for cilia anymore. *Curr. Opin. Cell Biol.* **22**, 75-80.
Batista, A., Millán, J., Mittelbrunn, M., Sánchez-Madrid, F. and Alonso, M. A. (2004). Recruitment of transferrin receptor to immunological synapse in response to TCR engagement. *J. Immunol.* **172**, 6709-6714.
Bonello, G., Blanchard, N., Montoya, M. C., Aguado, E., Langlet, C., He, H. T., Nunez-Cruz, S., Malissen, M., Sanchez-Madrid, F., Olive, D. et al. (2004). Dynamic recruitment of the adaptor protein LAT: LAT exists in two distinct intracellular pools and controls its own recruitment. *J. Cell Sci.* **117**, 1009-1016.
Capitani, N., Patrussi, L., Trentin, L., Lucherini, O. M., Cannizzaro, E., Migliaccio, E., Frezzato, F., Gattazzo, C., Forconi, F., Pelicci, P. et al. (2012). S1P1 expression is controlled by the pro-oxidant activity of p66Shc and is impaired in B-CLL patients with unfavorable prognosis. *Blood* **120**, 4391-4399.
Das, V., Nal, B., Dujeancourt, A., Thoulouze, M. I., Galli, T., Roux, P., Dautry-Varsat, A. and Alcover, A. (2004). Activation-induced polarized recycling targets T cell antigen receptors to the immunological synapse; involvement of SNARE complexes. *Immunity* **20**, 577-588.
Ehrlich, L. I., Ebert, P. J., Krummel, M. F., Weiss, A. and Davis, M. M. (2002). Dynamics of p56lck translocation to the T cell immunological synapse following agonist and antagonist stimulation. *Immunity* **17**, 809-822.
Finetti, F. and Baldari, C. T. (2013). Compartmentalization of signaling by vesicular trafficking: a shared building design for the immune synapse and the primary cilium. *Immunol. Rev.* **251**, 97-112.
Finetti, F., Paccani, S. R., Riparbelli, M. G., Giacomello, E., Perinetti, G., Pazour, G. J., Rosenbaum, J. L. and Baldari, C. T. (2009). Intraflagellar transport is required for polarized recycling of the TCR/CD3 complex to the immune synapse. *Nat. Cell Biol.* **11**, 1332-1339.
Follit, J. A., Tuft, R. A., Fogarty, K. E. and Pazour, G. J. (2006). The intraflagellar transport protein IFT20 is associated with the Golgi complex and is required for cilia assembly. *Mol. Biol. Cell* **17**, 3781-3792.
Follit, J. A., Xu, F., Keady, B. T. and Pazour, G. J. (2009). Characterization of mouse IFT complex B. *Cell Motil. Cytoskeleton* **66**, 457-468.
Fooksman, D. R., Vardhana, S., Vasiliver-Shamis, G., Liese, J., Blair, D. A., Waite, J., Sacristán, C., Victora, G. D., Zanin-Zhorov, A. and Dustin, M. L. (2010). Functional anatomy of T cell activation and synapse formation. *Annu. Rev. Immunol.* **28**, 79-105.
Gerdes, J. M., Liu, Y., Zaghloul, N. A., Leitch, C. C., Lawson, S. S., Kato, M., Beachy, P. A., Beales, P. L., DeMartino, G. N., Fisher, S. et al. (2007). Disruption of the basal body compromises proteasomal function and perturbs intracellular Wnt response. *Nat. Genet.* **39**, 1350-1360.
Gomez, T. S. and Billadeau, D. D. (2009). A FAM21-containing WASH complex regulates retromer-dependent sorting. *Dev. Cell* **17**, 699-711.
Gorska, M. M., Liang, Q., Karim, Z. and Alam, R. (2009). Uncoordinated 119 protein controls trafficking of Lck via the Rab11 endosome and is critical for immunological synapse formation. *J. Immunol.* **183**, 1675-1684.
Hutagalung, A. H. and Novick, P. J. (2011). Role of Rab GTPases in membrane traffic and cell physiology. *Physiol. Rev.* **91**, 119-149.
Iezzi, G., Karjalainen, K. and Lanzavecchia, A. (1998). The duration of antigenic stimulation determines the fate of naive and effector T cells. *Immunity* **8**, 89-95.
Jékely, G. and Arendt, D. (2006). Evolution of intraflagellar transport from coated vesicles and autogenous origin of the eukaryotic cilium. *Bioessays* **28**, 191-198.
Jin, H., White, S. R., Shida, T., Schulz, S., Aguiar, M., Gygi, S. P., Bazan, J. F. and Nachury, M. V. (2010). The conserved Bardet-Biedl syndrome proteins assemble a coat that traffics membrane proteins to cilia. *Cell* **141**, 1208-1219.
Keady, B. T., Le, Y. Z. and Pazour, G. J. (2011). IFT20 is required for opsin trafficking and photoreceptor outer segment development. *Mol. Biol. Cell* **22**, 921-930.
Kumar, A., Kremer, K. N., Dominguez, D., Tadi, M. and Hedin, K. E. (2011). Gα13 and Rho mediate endosomal trafficking of CXCR4 into Rab11+ vesicles upon stromal cell-derived factor-1 stimulation. *J. Immunol.* **186**, 951-958.
Larghi, P., Williamson, D. J., Carpier, J. M., Dogniaux, S., Chemin, K., Bohineust, A., Danglot, L., Gaus, K., Galli, T. and Hivroz, C. (2013). VAMP7

controls T cell activation by regulating the recruitment and phosphorylation of vesicular Lat at TCR-activation sites. *Nat. Immunol.* **14**, 723-731.
Li, X. and Donowitz, M. (2008). Fractionation of subcellular membrane vesicles of epithelial and nonepithelial cells by OptiPrep density gradient ultracentrifugation. *Methods Mol. Biol.* **440**, 97-110.
Lim, S. N., Bonzelius, F., Low, S. H., Wille, H., Weimbs, T. and Herman, G. A. (2001). Identification of discrete classes of endosome-derived small vesicles as a major cellular pool for recycling membrane proteins. *Mol. Biol. Cell* **12**, 981-995.
Liu, H., Rhodes, M., Wiest, D. L. and Vignali, D. A. (2000). On the dynamics of TCR:CD3 complex cell surface expression and downmodulation. *Immunity* **13**, 665-675.
Manders, E. M., Stap, J., Brakenhoff, G. J., van Driel, R. and Aten, J. A. (1992). Dynamics of three-dimensional replication patterns during the S-phase, analysed by double labelling of DNA and confocal microscopy. *J. Cell Sci.* **103**, 857-862.
Margadant, C., Kreft, M., de Groot, D. J., Norman, J. C. and Sonnenberg, A. (2012). Distinct roles of talin and kindlin in regulating integrin α5β1 function and trafficking. *Curr. Biol.* **22**, 1554-1563.
Maxfield, F. R. and McGraw, T. E. (2004). Endocytic recycling. *Nat. Rev. Mol. Cell Biol.* **5**, 121-132.
Mayle, K. M., Le, A. M. and Kamei, D. T. (2012). The intracellular trafficking pathway of transferrin. *Biochim. Biophys. Acta* **1820**, 264-281.
Omori, Y., Zhao, C., Saras, A., Mukhopadhyay, S., Kim, W., Furukawa, T., Sengupta, P., Veraksa, A. and Malicki, J. (2008). Elipsa is an early determinant of ciliogenesis that links the IFT particle to membrane-associated small GTPase Rab8. *Nat. Cell Biol.* **10**, 437-444.
Pampliega, O., Orhon, I., Patel, B., Sridhar, S., Díaz-Carretero, A., Beau, I., Codogno, P., Satir, B. H., Satir, P. and Cuervo, A. M. (2013). Functional interaction between autophagy and ciliogenesis. *Nature* **502**, 194-200.
Patino-Lopez, G., Dong, X., Ben-Aissa, K., Bernot, K. M., Itoh, T., Fukuda, M., Kruhlak, M. J., Samelson, L. E. and Shaw, S. (2008). Rab35 and its GAP EPI64C in T cells regulate receptor recycling and immunological synapse formation. *J. Biol. Chem.* **283**, 18323-18330.
Patrussi, L., Ulivieri, C., Lucherini, O. M., Paccani, S. R., Gamberucci, A., Lanfrancone, L., Pelicci, P. G. and Baldari, C. T. (2007). p52Shc is required for CXCR4-dependent signaling and chemotaxis in T cells. *Blood* **110**, 1730-1738.
Pazour, G. J. and Bloodgood, R. A. (2008). Targeting proteins to the ciliary membrane. *Curr. Top. Dev. Biol.* **85**, 115-149.
Pazour, G. J., Baker, S. A., Deane, J. A., Cole, D. G., Dickert, B. L., Rosenbaum, J. L., Witman, G. B. and Besharse, J. C. (2002). The intraflagellar transport protein, IFT88, is essential for vertebrate photoreceptor assembly and maintenance. *J. Cell Biol.* **157**, 103-114.
Pedersen, L. B. and Rosenbaum, J. L. (2008). Intraflagellar transport (IFT) role in ciliary assembly, resorption and signalling. *Curr. Top. Dev. Biol.* **85**, 23-61.
Pérez-Martínez, M., Gordón-Alonso, M., Cabrero, J. R., Barrero-Villar, M., Rey, M., Mittelbrunn, M., Lamana, A., Morlino, G., Calabia, C., Yamazaki, H. et al. (2010). F-actin-binding protein drebrin regulates CXCR4 recruitment to the immune synapse. *J. Cell Sci.* **123**, 1160-1170.
Qin, H., Wang, Z., Diener, D. and Rosenbaum, J. (2007). Intraflagellar transport protein 27 is a small G protein involved in cell-cycle control. *Curr. Biol.* **17**, 193-202.
Salmerón, A., Borroto, A., Fresno, M., Crumpton, M. J., Ley, S. C. and Alarcón, B. (1995). Transferrin receptor induces tyrosine phosphorylation in T cells and is physically associated with the TCR zeta-chain. *J. Immunol.* **154**, 1675-1683.
Schafer, J. C., Winkelbauer, M. E., Williams, C. L., Haycraft, C. J., Desmond, R. A. and Yoder, B. K. (2006). IFTA-2 is a conserved cilia protein involved in pathways regulating longevity and dauer formation in Caenorhabditis elegans. *J. Cell Sci.* **119**, 4088-4100.
Sedmak, T. and Wolfrum, U. (2010). Intraflagellar transport molecules in ciliary and nonciliary cells of the retina. *J. Cell Biol.* **189**, 171-186.
Soares, H., Henriques, R., Sachse, M., Ventimiglia, L., Alonso, M. A., Zimmer, C., Thoulouze, M. I. and Alcover, A. (2013). Regulated vesicle fusion generates signaling nanoterritories that control T cell activation at the immunological synapse. *J. Exp. Med.* **210**, 2415-2433.
Sönnichsen, B., De Renzis, S., Nielsen, E., Rietdorf, J. and Zerial, M. (2000). Distinct membrane domains on endosomes in the recycling pathway visualized by multicolor imaging of Rab4, Rab5, and Rab11. *J. Cell Biol.* **149**, 901-914.
Vardhana, S., Choudhuri, K., Varma, R. and Dustin, M. L. (2010). Essential role of ubiquitin and TSG101 protein in formation and function of the central supramolecular activation cluster. *Immunity* **32**, 531-540.
Wood, C. R., Huang, K., Diener, D. R. and Rosenbaum, J. L. (2013). The cilium secretes bioactive ectosomes. *Curr. Biol.* **23**, 906-911.
Yudushkin, I. A. and Vale, R. D. (2010). Imaging T cell receptor activation reveals accumulation of tyrosine-phosphorylated CD3ζ in the endosomal compartment. *Proc. Natl. Acad. Sci. USA* **107**, 22128-22133.